Deutscher Luft- und Raumfahrtkongress 2009
DocumentID: 121212

# ARIANE 5 RECOVERY BOOSTER FEM ANALYSES - VERIFICATION OF WATER IMPACT LOAD EVENTS

Dipl.-Ing. M. Groenewolt, Dr.-Ing. G. Schullerer,
MT-Aerospace, Franz-Josef-Strauß-Str. 5, Germany

**Abstract**

ARIANE 5 flight L537 took place on August 15th 2007. It was the third successful flight with a Booster where the cylinders of the segments were welded together. For this flight it was intended to recover the Boosters in order to verify the quality and reliability after the application of the whole load history. The periodic A5 EAP recovery for expertise are performed in the frame of the ARTA program, an ESA program managed in cooperation with CNES which acts as ESA 'Assistant Maîtrise d'ouvrage'.
The segment 3 of the recovered Booster showed a large irreversible deformation field. MT Aerospace as the manufacturer of the CPN/S-Booster was asked by EUP for an expertise to predict those load state which is responsible for the generation of the observed deformation field.
This paper presents the methods and results of the non-linear analyses. The prediction, which is based on a finite element model including contact formulation, is compared with the observed buckle of the recovered segment. On the basis of the measured deformation pattern it could be clearly shown that the appearance of the irreversible deformation is caused by water impact. The event of cavity collapse during water impact after re-entry could be identified as the relevant loading situation.

## 1. GENERAL

### 1.1. Structure Identification

The purpose of the solid propellant Booster on ARIANE 5 (see Figure 1) is to produce the main lift during the first 110s. The Boosters store 241t of solid propellant and consists out of three segments which are joined via sealed clevis tang connections. The metallic Booster is fabricated by flow turning.
Its principal components of interest concerning the buckling analyses are:

a) The lower segment 3, in which the buckle occurred, consists out of three cylinders and the aft dome welded together to one segment.
b) The metallic ring (DAAR) which is situated at segment 3 and connects the Booster with the main stage. It assures that the EAP is constrained in lateral position.

### 1.2. Booster Recovery

Periodically a Booster is recovered by ship from the Atlantic Ocean after reentry for analyses purpose (the Boosters are not meant to be reused). This is done to ensure production quality and to detect eventual anomalies occurring during mission. The analysis on hand concerns the first welded recovered booster which showed a large irreversible deformation after recovering in the lower part of segment three. An analysis of the parachute system showed that the predicted impact velocity was exceeded due to a malfunction and a reduced deployment of the parachute. The impact s by the trajectory analysis lead to distinctively higher predictions.

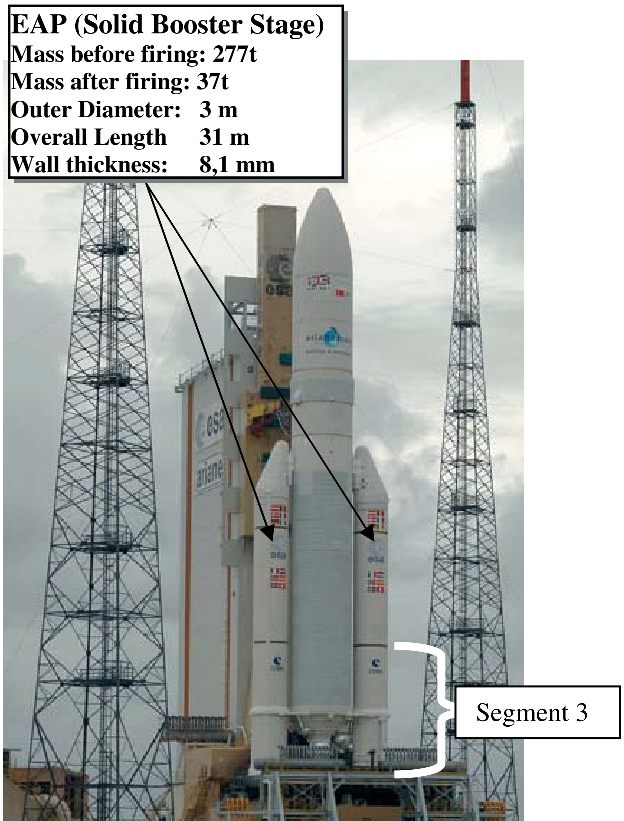


**Figure 1 Solid propellant boosters attached to the ARIANE 5 main stage.**

## 2. THE OBSERVED DEFORMATION

Figure 2 shows the buckled booster after water impact. An irreversible deformation of the last cylinder can be seen and the nozzle is also missing. MT-A as the manufacturer of the booster case was therefore asked to perform analyses concerning the buckle in cylinder V7. The objective was to assure the thesis that the water impact has caused the booster to buckle in the observed way.

**Figure 2 Buckled Booster after recovering from Ocean (original photo by CNES)**

## 3. ANALYSIS STRATEGY

The impact of the booster into the water is a quite complex event and could therefore not be simulated directly, because the construction of a mathematical model would be too cost and time intensive and a validation would not be possible without an extensive test program. In addition no exact information about the impact parameters like impact velocity in horizontal- and vertical direction, angle or waves is available. So some simplifications have to be done concerning the simulation of the damaging load event and the following strategy was chosen:

a) Translation of the justified Finite Element MARC model to ABAQUS
b) Verification of the translation with a number of checks, including Eigenfrequency- and linear buckling analyses with a test load
c) Analyzing different reasonable static load conditions
d) Comparison of the found buckling pattern with the real buckle
e) Comparison of the found load magnitude with measurements by NASA

## 4. MATHEMATICAL MODEL

### 4.1. Modeled Structural Components

The model used for Booster buckling load analyses includes the following main structural components:

a) A simplified DAAR ring
b) segment 3 consisting out of three cylinders and one dome welded together, including all changes in wall thickness due to weld interfaces and aft dome

The model is based on an already existing and justified model. Because of the not known load conditions a 360° model was generated.

### 4.2. Geometric Properties

The segment was modeled with nominal wall thickness. The DAAR was simplified by a U-profile with the appropriate wall thickness.

### 4.3. Material Properties

The material model of the booster (D6AC steel) is characterized by isotropic elastic-plastic behavior with isotropic strain hardening (v. Mises plasticity). The hardening is described by the Ramberg-Osgood equation. A selection of applied material parameters is summarized in Table 1.

| D6AC Steel at 150° | | | |
|---|---|---|---|
| Yield Strength (tension) | $R_{p0.2}$ | [MPa] | 1017 |
| Tensile Strength | $R_m$ | [MPa] | 1764 |
| Young's Modulus | E | [MPa] | 193154 |
| Poisson's Ratio | $\nu$ | [ ] | 0.3 |

**Table 1 Material data of the booster steel at 150°C**

### 4.4. Boundary Conditions

The nodes on the upper interface to segment 2 are fixed in all three translational degrees of freedom.

## 5. FINITE ELEMENT MODELING

### 5.1.1. Software

The Model was created in MarcMentat2007r1 and then transferred to ABAQUS. All further analyses were performed with ABAQUS 6.7-EF.

### 5.1.2. Discretisation

The finite element model uses a separate mesh for segment 3 and the simplified DAAR. For segment 3 second-order reduced integration shell element formulation (S8R) was used and for the DAAR Ring 4 node reduced integration shell element formulations (S4R) are chosen, because of better contact interaction properties.
The problem statistics is summarized as follows:

| Structural Part | Element Type | Elements | Nodes |
|---|---|---|---|
| S3 | S8R | 39120 | 117840 |
| DAAR | S4R | 1962 | 2180 |

#### 5.1.3. Analysis Parameters

Because of large displacements during buckling geometric nonlinearity is taken into account.

#### 5.1.4. Contact between DAAR Ring and Segment 3

Between DAAR Ring and Segment 3 a contact constraint is set. Hard contact was chosen together with the automatic contact tolerance option in ABAQUS.

### 5.2. Verification of the model

To verify the model, crosschecks between the already qualified MARC model and the ABAQUS model have been performed. This included:

a) A frequency analyses
b) A linear buckling analyses with non uniform axial load

All 26 calculated Eigenmodes and Eigenvalues of the frequency analyses show full compliance. Figure 3 shows exemplarily the first Eigenmode for both analyses and the mode as well as the Eigenfrequency do match well.
Furthermore linear buckling analyses with gauss distributed test loads were performed. Again the results do match well for all calculated buckling modes, see exemplarily Figure 4. Therefore the translated ABAQUS model is justified by verification with the qualified MARC model.

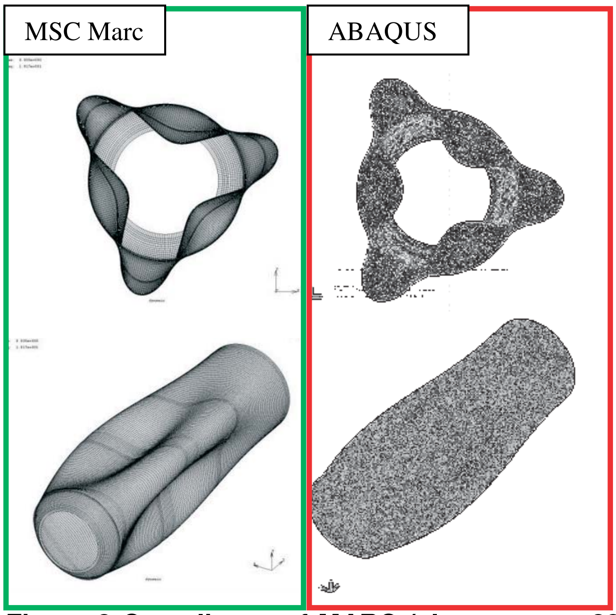


**Figure 3 Compliance of MARC (element-type 22) Mode 1 and associated Eigenfrequency with ABAQUS (element-type S8R) Mode 1**

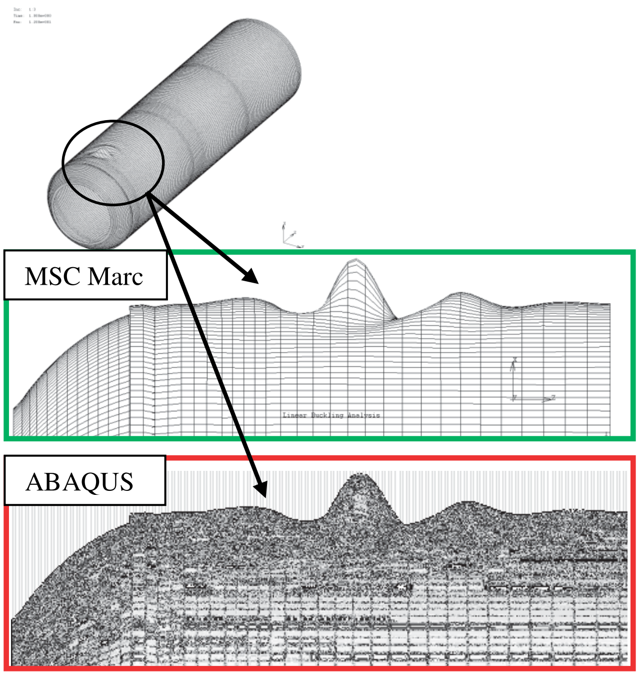


**Figure 4 Comparison of the ABAQUS and MARC results for Buckling mode 3; compliance in predicted buckling load factor**

## 6. RESULTS

### 6.1. Chosen analyses approach and estimation of the influence of the artificial damping energy

The static non linear analysis shows sudden convergence difficulties when reaching the onset of the local deformation. An adequate way to smooth severe discontinuities is to add viscous damping energy. To ensure that the effect on the results is small, the damping energy was compared with the total strain energy. Figure 5 shows that the total energy dissipated due to stabilization is small compared to the total energies involved in deformation. This ensures that the results are not influenced significantly by the viscous damping. In addition, calculations with different amounts of viscous damping have been performed. It was also possible to analyse the deformation without any stabilisation energy but then the time increments become very small. The difference in maximum deformation at the evaluation time between the calculation with small damping energy and the analyses without damping is smaller than 1.6%, but the analyses without stabilization needs almost twice as much cpu time. Therefore the analyses were performed with a small amount of stabilization energy, accounting also for the actual water impact, where water would produce a certain amount of damping as well as the inertia of the structure.

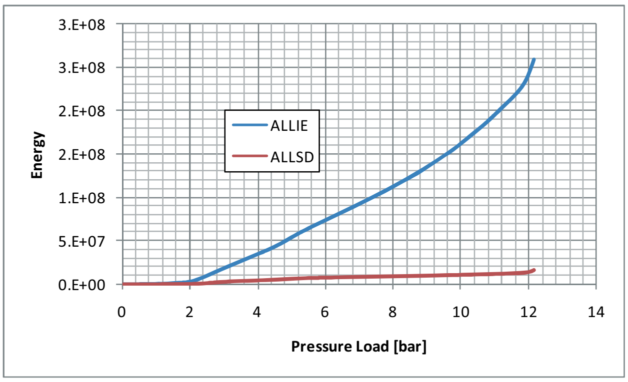


**Figure 5 Stabilization energy (ALLSD) vs. total dissipated energy (ALLIE)**

### 6.2. Identified load condition which was responsible for the deformation

A number of reasonable load conditions have been analyzed and it was possible to identify a load combination which results in the observed deformations. The post predicted deformation field shows excellent agreement with the real deformation pattern. Magnitude as well as dimension and geometry of the buckle do match with the deformation in the lower segment, see Figure 8.
Also the distribution of the buckle underneath the DAAR ring could be predicted accurately, refer to Figure 9.

The identified load condition is governed by a radial external pressure on the cylinder wall, see

Figure 6.
This loading situation leads to the conclusion that it was not the initial impact of the booster into the water which caused the deformation at segment 3 by loading the booster in axial direction due to the deceleration.

Instead the deformation was caused by an external pressure due to a load event which occurs after the initial impact and is caused by cavity collapse.
As the booster dips into the ocean a cavity forms around it and collapses after a short time. This load causes distinctive external pressure peaks in the lower part of the booster.

The found magnitude as well as the external pressure distribution is completely in common with measurements of cavity collapse pressure performed by NASA for the shuttle booster.

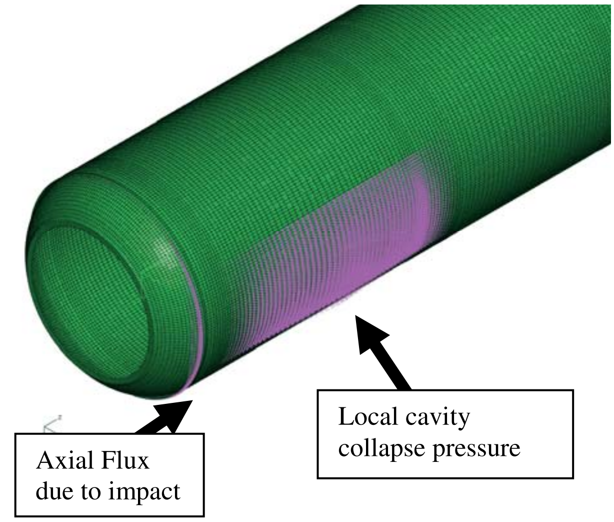


**Figure 6 Loading conditions which leads to the observed buckle**

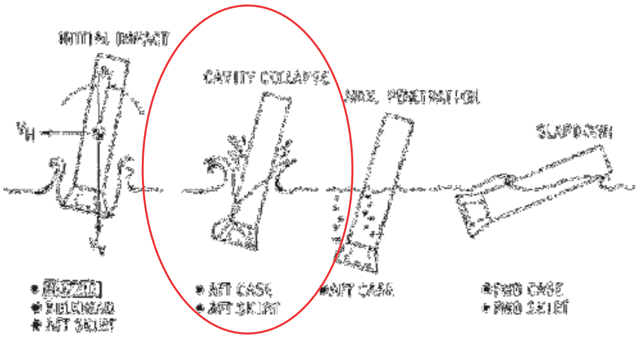


**Figure 7 Load phases due to water impact [R2]**

## 7. CONCLUSION

On the basis of measured deformation pattern it is verified that the appearance of the irreversible deformation was caused by water impact. The relevant load condition could be identified as the cavity collapse external pressure and the occurring deformation field could be simulated.

## 8. REFERENCES

[1] Hibbit, Karlsson & Sorensen, “ABAQUS User´s and Example Problems Manual, Version 6.6”, HKS, Inc., Pawtucket, R.I., USA, 2004.

[2] R.S. Ryan et al, “System Analyses Approach to Deriving Design Criteria (Loads) for Space Shuttle and Its Payloads Volume II – Typical Examples”, George C. Marshall Space Flight Center, Alabama, USA, 1981.

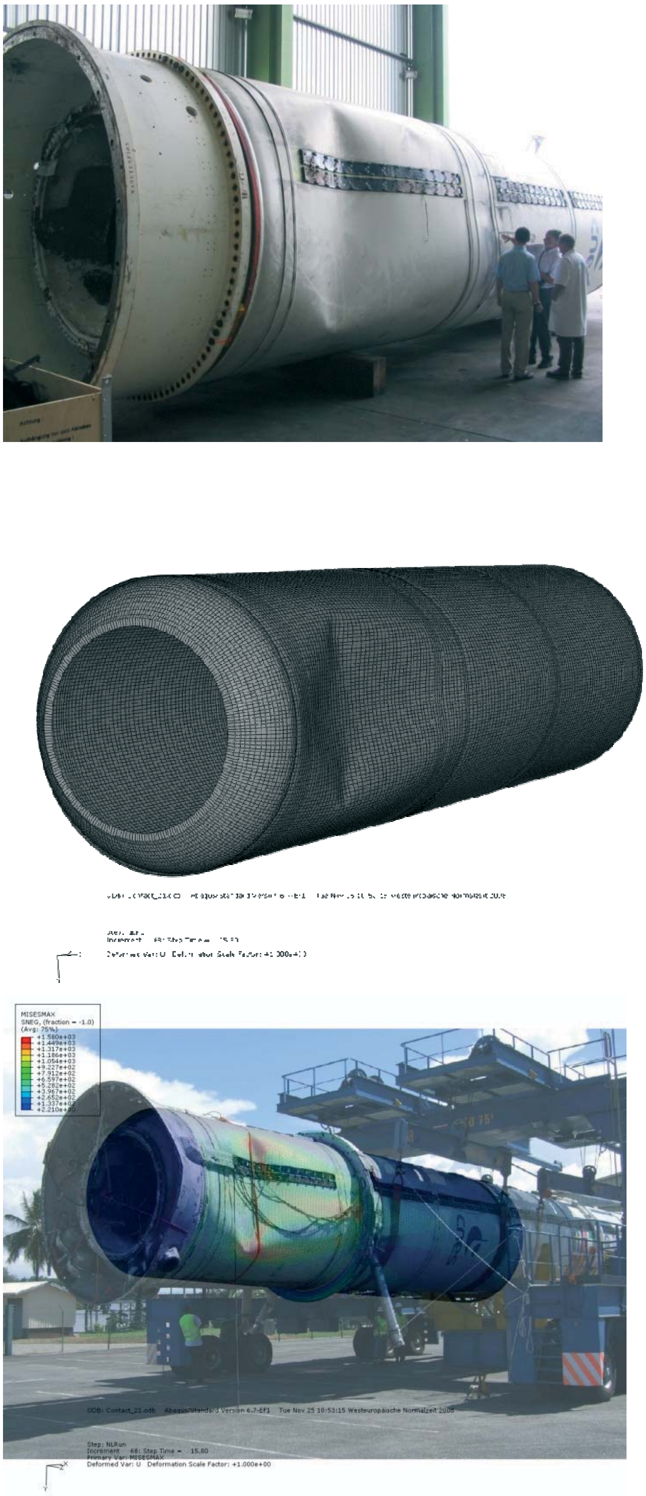

**Figure 8 Qualitative comparison of the prediction with the real deformation pattern (original photo by CNES).**

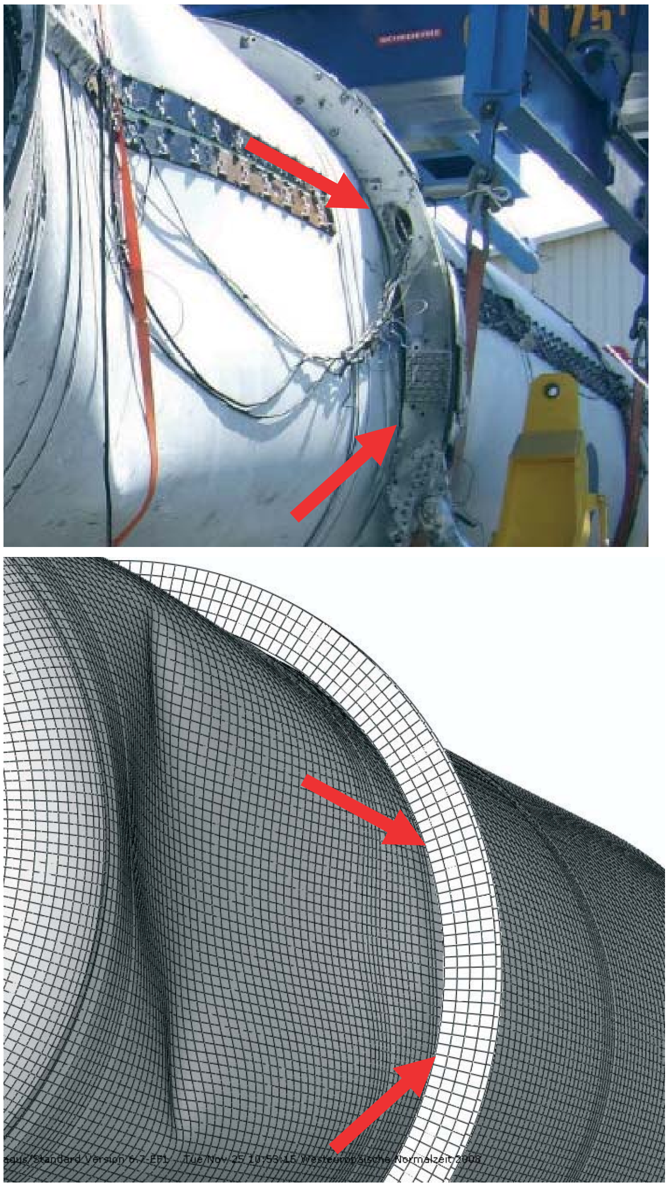

**Figure 9 Buckle distributing underneath the DAAR ring (original photo by CNES).**